Reduction of multipath effect through a critical scattering zone in microcell environments

C.A. López Miranda
Wireless Communications Group
CICESE RESEARCH CENTER
Km. 107 Carretera Tijuana-Ensenada,
Ensenada Baja California 22860 México
Tel (52+646) 1745050, Fax (52+646) 1750554,
e-mail: clopez@cicese.mx
Also, with the Universidad de Sonora, Mexico

D.H. Covarrubias Rosales
Wireless Communications Group
CICESE RESEARCH CENTER,
e-mail: dacoro@cicese.mx

Recibido el 2 de agosto de 204; aceptado el 20 de septiembre de 2005

In this work, we investigate a critical region (CR) in microcell elliptical environments, an area between the mobile and the base station (BS) containing multipaths whose angles and times of arrival possess the acceptable angle and delay spreads of the channel. The focus of the paper is to estimate the theoretical rates of multipath reduction expected from the CR. These rates illustrate the convenience of adjusting or not the antenna's beamwidth (aperture) according to the angle spread. Also, to confirm the model's results; the angle and time of arrival statistics deduced from the elliptical model are validated through simulation. Results closely agree with theoretical values expected from the model.

Keywords: Multipath effect; microcell; critical region; statistical analysis; antenna aperture.

En este trabajo, investigamos una región crítica (CR) en entornos elípticos microcelulares, una área entre el móvil y la estación base (BS) que contiene las multitrayectorias cuyos ángulos y tiempos de arribo poseen un esparcimiento angular y temporal aceptable del canal. El trabajo se enfoca en estimar la proporción teórica de la reducción de multitrayectorias esperadas de la RC. Estas razones ilustran la conveniencia o no de ajustar el ancho de haz de la antena (apertura) de acuerdo al esparcimiento angular. Para confirmar los resultados del modelo, las estadísticas generadas a través del modelo elíptico para el ángulo y tiempo de arribo son validadas por simulación. Los resultados concuerdan con los valores teóricos esperados del modelo.

Descriptores: Angle spread; elliptical model; microcell; multipath.

PACS: 41.20.Jb; 42.68.Ay; 42.25.Fx

1. Introduction

To minimize the undesirable effects of fading, multipath, and co-channel interference of wireless communications systems using antenna arrays or directional antennas, it is necessary to analyze the spatial characteristics of the environment through channel models, in order to obtain measurements of the angle spread (AS) and delay spread (DS) relative to the signal impinging on the base station (BS). Several works have focused on channel modeling according to the angle of arrival (AOA) and time of arrival (TOA) [1-6]. Janaswamy presents a statistical Gaussian model for microcell and macrocell environments [1]. Ertel and Reed in Ref. 2 and Liberti and Rappaport in Ref. 3 developed a microcell statistical channel model, named the Geometrically Based Single Bounce Elliptical Model (GBSBEM). The GBSBEM model provides the statistics of the AOA and TOA, which are useful in predicting the performance of an array of antennas. Also these statistics are used in this paper to illustrate the amount of multipath reduction arising from outside the CR. Therefore, the knowledge of the rate of scatterers (objects in the environment where the signal is reflected, such as building and trees) coming from the CR is very important. The GBSBEM is applicable to microcell environments, in cases where the BS´s antenna can be at the same height as the surrounding objects or when the antenna's height is low, and when the mobile-BS distance can be up to 3 kilometers. In those cases, the AS of the received signal at the BS is larger than in the macrocell scenarios; this is because the scattering process also occurs in the vicinity of the BS. Practical measurements of the AS, ranging from 6 to 54.2 degrees for several cities, are reported in Refs. 7 and 8, showing that the AS depends on both the antenna's height and the scattering environment.

Section 2 presents general considerations of the elliptical model and defines those conditions that characterize the CR. Numerical statistics corresponding to the CR, validation of the GBSBEM model and discussion of results are presented in Sec. 3. Section 4 contains the conclusion.

2. Critical scattering region

2.1. Model assumption and statistics of the AOA and the TOA

The GBSBEM model assumes that scatterers are uniformly distributed within an elliptical area surrounding the transmitter and receiver, in which the BS and the mobile station are the ellipse's foci [2]. A typical microcell elliptical scenario is shown in Fig. 1. For the purpose of analysis, the coordinate system can be conveniently selected as the (x, y) plane, so that the mobile and the BS are located along the x-axis. The ellipse's dimensions are defined by threshold time τ_m and focal distance D, where only multipath signals with TOA, denoted by τ, such that $\tau \leq \tau_m$, are accounted for by the model. The parameters a_m and b_m, given in 1, are the semimajor and semiminor axes of the ellipse containing the scatterers.

$$a_m = \frac{c\tau_m}{2} \quad \text{and} \quad b_m = \frac{\sqrt{c^2\tau_m^2 - D^2}}{2}, \tag{1}$$

where c is the speed of light and D represents the distance between the mobile and the BS. Thus, every signal coming from outside the ellipse will be omitted because it exceeds the level of acceptable attenuation due to its TOA (grater than the acceptable maximum time (τ_m).

The physical conditions are as follows. The radiation patterns for both the transmitter and the receiver antennas are assumed to be omnidirectional. Since the heights of the antennas and the scatterers are alike, a two dimensional propagation model can be considered in the azimuthal plane. The scatterers are assumed to be omnidirectional re-radiating elements with equal scattering coefficients, but phases are considered to be independent

Since we are concerned with the AS and DS of the channel, which depend on the mean and standard deviation of the AOA and TOA, respectively, first we present the probability density functions (pdf's) derived in Ref. 2 for such parameters. The AOA pdf observed at the BS can be derived from the joint pdf $f_{r,\theta}(r, \theta)$ regarding to a point in polar coordinates (r, θ), where θ represents the AOA at the BS and $r > 0$ stands for the distance between the scatter (x, y) and the BS. The pdf $f_{r,\theta}(r, \theta)$ can be obtained from the spatial distribution pdf $f_{x,y}(x, y)$ of the scatterers by using the Jacobian of the transformation [6] between the Cartesian and Polar coordinates; this fact is shown in (2), where the Jacobian (J) is expressed by r. Due to the uniform distribution of scatterers,

$$f_{x,y}(x, y) = \frac{1}{A_e},$$

where A_e is the area given of the ellipse by $\pi a_m b_m$:

$$f_{r,\theta}(r, \theta) = r f_{x,y}(x, y) \Big|_{\substack{x = r\cos\theta \\ y = r\sin\theta}} \tag{2}$$

Hence, the marginal AOA pdf becomes

$$f_\theta(\theta) = \int_0^{r_e} f_{r,\theta}(r, \theta)dr = \frac{1}{8\pi a_m b_m}\left(\frac{D^2 - \tau_m^2 c^2}{D\cos\theta - \tau_m c}\right)^2 \quad -\pi \leq \theta \leq \pi. \tag{3}$$

Note in (3), that for a given fixed angle θ, the value r is limited by the ellipse (polar equation)

$$r_e = (D^2 - \tau_m^2 c^2)/2(D\cos\theta - \tau_m c)$$

representing the scattering region [2]. From symmetry, the mean angle $\bar{\theta}$ is zero and the angular standard deviation σ_θ is

$$\sigma_\theta = \left[\int_{-\pi}^{\pi} \theta^2 f_\theta(\theta)\mathrm{d}\theta\right]^{\frac{1}{2}} \tag{4}$$

$$\sigma_\theta = \left[\frac{\pi^2}{3} + \frac{4b_m}{a_m}\ln\left(\frac{2a_m + 2b_m}{2a_m + 2b_m + D}\right) + 4\sum_{n=1}^{\infty}\left(\frac{-D}{2a_m + 2b_m}\right)^n \frac{1}{n^2}\right]^{\frac{1}{2}}. \tag{5}$$

The integral (4) is obtained by using the Parserval's theorem and the Fourier coefficients of $f_\theta(\theta)$. A complete development of (5) is presented in Janaswamy [6, see Eqs. 6.5 and 6.24].

To get the TOA pdf, $f_\tau(\tau)$, we start from the cumulative density function (cdf) $F_\tau(\tau)$ and then take

$$f_\tau(\tau) = dF_\tau(\tau)/d\tau.$$

As the scatterers are uniformly distributed, the cdf is directly $F_\tau(\tau) = A(\tau)/A_e$, where $A(\tau)$ is the area of intersection between the ellipse associated with a TOA τ and the ellipse associated with τ_m. In this case, $A(\tau)$ is the area of the first ellipse itself, so that $A(\tau) = \pi a(\tau)b(\tau)$, where $a(\tau)$ and $b(\tau)$ are found from (1), taking $\tau = \tau_m$, $a = a_m$ and $b = b_m$. Thus, the cdf turns out to be

$$F_\tau(\tau) = \frac{\tau c\sqrt{c^2\tau^2 - D^2}}{4a_m b_m}. \tag{6}$$

Consequently, the marginal pdf (obtained from $dF/d\tau$), mean TOA ($\bar{\tau}$) and the standard deviation (σ_τ) of τ are given

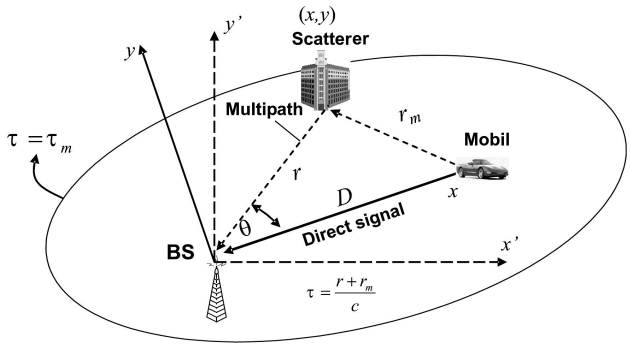

FIGURE 1. Typical microcell scenario used by the elliptical model.

by 7, 8 and 9, respectively. A complete development of the formulae of $\bar{\tau}$ and σ_τ can be found in [6, see Eqs. 6.27 and 6.28]:

$$f_\tau(\tau)=\frac{c(2\tau^2c^2-D^2)}{4a_mb_m\sqrt{\tau^2c^2-D^2}}, \quad \frac{D}{c}\leq\tau\leq\tau_m \tag{7}$$

$$\bar{\tau}=\frac{1}{4a_mb_m}\left[\frac{D^2(\tau_m^2c^2-D^2)^{\frac{1}{2}}}{c}+\frac{2\left(\tau_m^2c^2-D^2\right)^{\frac{3}{2}}}{3c}\right] \tag{8}$$

$$\sigma_\tau=\left\{\begin{array}{l}\frac{D^4}{4a_mb_mc^2}\left\{\frac{3\tau_mc+(\tau_m^2c^2-D^2)^{\frac{1}{2}}}{4D^2}\right. \\ +\frac{\tau_mc(\tau_m^2c^2-D^2)^{\frac{3}{2}}}{2D^4} \\ \left.+\ \frac{1}{4}\ln\left|\frac{\tau_mc+(\tau_m^2c^2-D^2)^{\frac{1}{2}}}{D}\right|\right\}-\bar{\tau}^2\end{array}\right\}^{\frac{1}{2}}. \tag{9}$$

2.2. Definition of critical region

The CR is defined as that region of scatterers whose multipath's AOA and TOA are simultaneously within the intervals defined by (10), an area originating between the intersection of an elliptical belt, corresponding to the upper and lower limits of the DS, and an angular aperture region representing the AS:

$$\bar{\theta}-\sigma_\theta\leq\theta\leq\bar{\theta}+\sigma_\theta \quad \text{and} \quad \bar{\tau}-\sigma_\tau\leq\tau\leq\bar{\tau}+\sigma_\tau. \tag{10}$$

The first inequality in (10) defines the angular scattering region, while the second characterizes an elliptical belt.

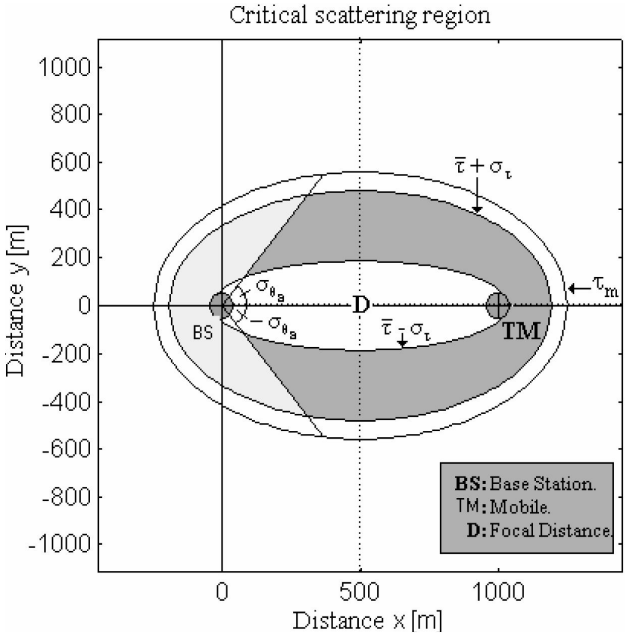

FIGURE 2. Critical scattering region based on the AS and DS (the physical area).

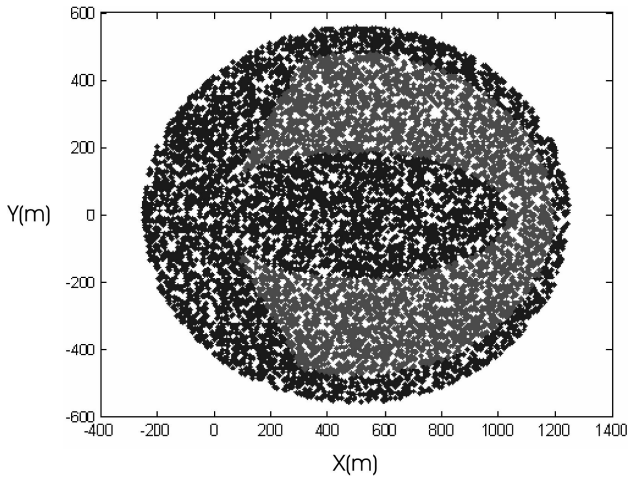

FIGURE 3. Set of simulated scatterers within the elliptical scenario and the CR.

3. Simulation results

Simulations are performed considering a microcell scenario by randomly placing 10,000 scatterers within an ellipse according to the threshold $\tau_m = 5\mu$s and $D = 1000$ m, which are suitable for microcell scenarios. Methods for selecting appropriate values of τ_m to achieve desired channel impulse response characteristics are given in [3]. The choice of τ_m determines both the DS and the AS of the channel, which are defined as twice their respective standard deviation, that is, $AS = 2\sigma_\theta$ and $DS = 2\sigma_\tau$. Thus, from 5, 8 and 9 we found $\bar{\theta} = 0, \sigma_\theta = 55.91°$, $\bar{\tau} = 4.08\mu$s and $\sigma_\tau = 0.53\mu$s. The large half AS value of $55.91°$ corresponds to a practical microcell environment when the height of the BS antenna is equal to or lower than the height of the buildings surrounding the BS. The CR is depicted in Fig. 2 according to the physical area; also the CR is shown in Fig. 3, using the set of 10,000 scatterers from the simulation.

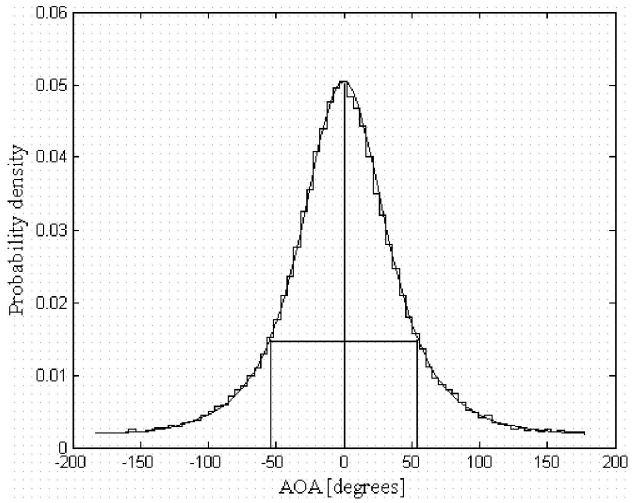

FIGURE 4. Comparison between the marginal AOA pdf and the normalized histogram.

3.1. Critical region statistics

The CR can be analyzed from three implicit events in 1, namely, a probability p_1 to find a scatterer inside the elliptical belt such that its TOA results in $\bar{\tau} - \sigma_\tau \leq \tau \leq \bar{\tau} + \sigma_\tau$; a probability p_2 relative to the angular region $\bar{\theta} - \sigma_\theta \leq \theta \leq \bar{\theta} + \sigma_\theta$; and a probability p_3 that a scatterer will belong to the CR. Note that the parameters p_1, p_2 and p_3 depend directly on the AS and the DS. Also, these parameters can be computed as follows:

$$p_1 = Pr[\bar{\tau} - \sigma_\tau \leq \tau \leq \bar{\tau} - \sigma_\tau] = F_\tau(4.62\mu s) - F_\tau(3.35\mu s) = 0.7287 \tag{11}$$

$$p_2 = \int_{-\sigma_\theta}^{+\sigma_\theta} f_\theta(\theta)d\theta = \int_{-\sigma_\theta}^{+\sigma_\theta} \frac{1}{8\pi a_m b_m}\left(\frac{\tau_m^2 c^2 - D^2}{\tau_m c - D\cos\theta}\right)^2 d\theta = 0.7634 \tag{12}$$

$$p_3 = Pr[\bar{\theta} - \sigma_\theta \leq \theta \leq \bar{\theta} + \sigma_\theta, \bar{\tau} - \sigma_\tau \leq \tau \leq \bar{\tau} + \sigma_\tau] = \int_{-\sigma_\theta}^{\sigma_\theta} \int_{\bar{\tau}-\sigma_\tau}^{\bar{\tau}+\sigma_\tau} f_{\tau,\theta}(\tau,\theta)d\tau d\theta \tag{13}$$

$$p_3 = \int_{-55.91}^{55.91} \int_{3.53\times10^{-6}}^{4.62\times10^{-6}} f_{\tau,\theta}(\tau,\theta)d\tau d\theta = 0.4134, \tag{14}$$

where $f_{\tau,\theta}(\tau,\theta)$ is the joint pdf of TOA/AOA [2].

$$f_{\tau,\theta}(\tau,\theta) = \begin{cases} \frac{(D^2-\tau^2c^2)(D^2c-\tau^2c^3-2\tau c^2 D\cos\theta)}{4\pi a_m b_m (D\cos\theta-\tau c)^3}, & \frac{D}{c} \leq \tau \leq \tau_m, \theta \neq 0 \\ \frac{c(D+c)}{4\pi a_m b_m}, & \frac{D}{c} \leq \tau \leq \tau_m, \theta = 0 \end{cases} \tag{15}$$

which come from

$$f_{\tau,\theta}(\tau,\theta) = \left.\frac{f_{r,\theta}(r,\theta)}{|J(r,\theta)|}\right|_{r=\frac{D^2-\tau^2c^2}{2(D\cos\theta-\tau c)}}, \quad J(r,\theta) = \left|\frac{\partial r}{\partial \tau}\right|^{-1}, \tag{16}$$

where J is the Jacobian and r represent the ellipse corresponding to a time τ. The function $f_{\tau,\theta}(\tau,\theta)$ in 13 is taken from its first expression in 15 because the limits of integration do not include scatterers located along the segment between the ellipse's foci. Since the values of 12 and 14 cannot be obtained in a closed form, they were computed by numerical integration via Matlab.

3.2. Discussion of results

The value of $p_1 = 0.73$ indicates that 73 percent of the scatterers arise from the elliptical belt, whose TOAs range from 3.55 to 4.62 μs while the AOA will be in $[0, 2\pi]$ whereas $p_2 = 0.76$ stands for the rate of scatterers inside the critical angular interval. Therefore, if the antenna considers either the elliptical belt or the angular region, at most 27 percent of multipaths will be cancelled. Nevertheless, the number of scatterers inside the CR (where the better signals arise from) is 41 percent (p_3); that is, if the BS can adjust its antenna's aperture (main beam beamwidth of a directional antenna or adaptive array) to the AS and the DS, then it will be possible to insolate up to 59 percent of the multipaths. These results must be viewed not only as rates of scatterers to be eliminated, but as the signals arising from the CR which are less liable to fade. That is, signals from the CR have a better power profile and space-time correlation [1], leading to a better quality of service for the system.

On the other hand, to confirm the theoretical pdf's from the elliptical model and validate their AS and DS outcomes, we make a comparison between the pdf functions and their respective normalized histograms. Fig. 4 illustrates the

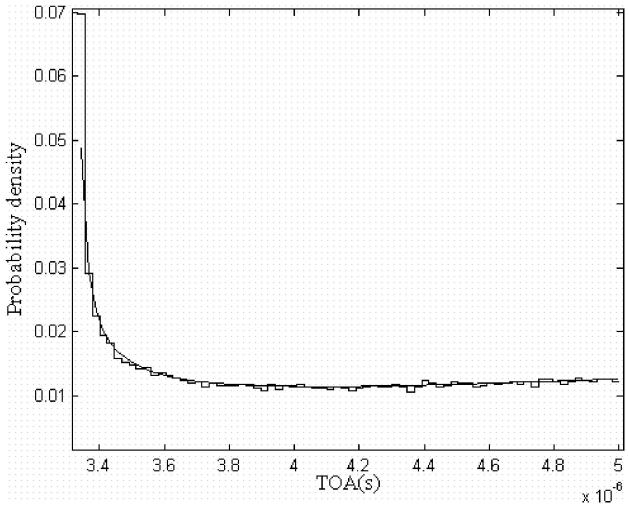

FIGURE 5. Comparison between the marginal TOA pdf and the normalized histogram.

pdf (3) and the normalized histogram related to the AOA, whereas Fig. 5 plots the pdf (7) and the normalized histogram related to the TOA. In both cases, simulated histograms closely match theoretical pdf´s. Hence, Figs. 4 and 5 can be seen as an empirical validation of the elliptical model, in which the AS and DS outcomes become to be appropriate for typical microcell scenarios [7,8] (as expected).

4. Conclusion

A CR useful for analyzing a cellular radio channel model was characterized. This characterization can be used to estimate the feasible rate of scatterers to be geographically isolated by the BS, as long as it has the capacity to adjust its aperture to the channel's AS and DS. The ratio of relevant multipaths arising from the CR was obtained for the microcell elliptical model. The amount of expected multipath reduction can be up to 59 percent. Furthermore, the model's results were validated through simulation, in which the parameters obtained from the model properly approach a typical microcell environment.

Acknowledgments

This work was supported by the Mexican National Science and Technology Council under Grant U39514-Y. Also, the author would like to thanks to the Universidad de Sonora that supports financially C.A. Lopez doctoral program at CICESE research center.

1. Ramakrishna Janaswamy, *IEEE Trans. On Wireless Communications* **1** (2002) 488.
2. R. Ertel and J. Reed, *Proc. IEEE JSAC* **17** (1999) 1829.
3. J.C. Liberti Jr. and T.S. Rappaport, *IEEE VTC* **xxx** (1996) 844.
4. P. Petrus, J.H. Reed, and T.S. Rappaport, *IEEE Trans. On Comms* **50** (2002) 495.
5. Ramakrishna Janaswamy, *Radiowave Propagation and Smart Antennas for Wireless Communications* (Kluwer Academic Publishers, 2001).
6. J.C. Liberti Jr. and T.S. Rappaport, *Smart Antennas for Wireless Communications: IS-95 and Third Generation CDMA Applications* (Prentice Hall PTR, 1999).
7. C. Cheon, G. Liang, and H.L. Bertoni, *IEEE JSAC* **19** (2001) 2191.
8. R.B. Ertel, P. Cardieri, K.V. Sowerby, T.S. Rappaport, and J.F. Reed, *IEEE Personal Communication* **xxx** (1998) 10.